

ON THE RELATIONSHIP BETWEEN MOMENT AND CURVATURE
FOR AN OVINE ARTERY

A Thesis

by

GABRIEL ALEJANDRO REZA

Submitted to the Office of Graduate Studies of
Texas A&M University
in partial fulfillment of the requirements for the degree of
MASTER OF SCIENCE

August 2006

Major Subject: Biomedical Engineering

ON THE RELATIONSHIP BETWEEN MOMENT AND CURVATURE
FOR AN OVINE ARTERY

A Thesis

by

GABRIEL ALEJANDRO REZA

Submitted to the Office of Graduate Studies of
Texas A&M University
in partial fulfillment of the requirements for the degree of

MASTER OF SCIENCE

Approved by:

Co-Chairs of Committee,	John C. Criscione
	K.R. Rajagopal
Committee Member,	William H. Hyman
Head of Department,	Gerard Cote

August 2006

Major Subject: Biomedical Engineering

ABSTRACT

On the Relationship Between Moment and Curvature
for an Ovine Artery. (August 2006)

Gabriel Alejandro Reza, B.S., Arizona State University

Co-Chairs of Advisory Committee: Dr. John C. Criscione
Dr. K.R. Rajagopal

To find a relationship between moment versus curvature in a traction-free ovine artery, a pure moment was applied to a radially cut ovine artery (length 50.23 mm). The curvature of the segment opposite the cut was calculated and used to calculate the pre-stresses using a Fung type model. The pre-stresses were then used to calculate the moment. The moment applied during the experiment was calculated by recording the twist applied and the stiffness of the wire applying the moment. The artery was sutured symmetrically with a custom jig, and then sutured to two blocks, one fixed and one subject to the pure moment. The axial strain was assumed unity. The Fung model yielded a linear moment versus curvature relationship, as well as the moment versus curvature relationship for the experiment. Despite both small and large stretches, the strains felt by the artery were not influential enough to display a non-linear correlation for moment vs curvature.

ACKNOWLEDGMENTS

I want to thank my committee, Dr. Criscione, Dr. Rajagopal, and Dr. Hyman for their support and guidance inside and outside of the classroom. I am lucky to have advisors that are so passionate about their work and teaching it to others.

I would like to thank my friends Craig, Art, Keho, and the department faculty and staff for helping me and making my experience memorable at Texas A&M. I'd like to thank the Texas A&M Veterinary School, and, especially my girlfriend, Kelley, for helping me obtain arteries to conduct this experiment.

Lastly, I would like to thank my family: Mom, Dad, Junior, Sophia, and Isabel for their endless source of support and love.

TABLE OF CONTENTS

CHAPTER		Page
I	INTRODUCTION	1
	A. Specific Aims	1
II	BACKGROUND	3
III	MATERIALS AND METHODS	7
	A. Physiological Salt Solution	7
	B. Equipment	7
	C. Artery Preparation	7
	D. Procedure	9
IV	CONSTITUTIVE ASSUMPTIONS AND KINEMATICS	18
V	MODELING THE EXPERIMENT	20
VI	RESULTS	25
VII	DISCUSSION AND CONCLUSION	32
	REFERENCES	35
	APPENDIX A	38
	APPENDIX B	45
	VITA	64

LIST OF TABLES

TABLE		Page
I	Data for the un-halved artery.	26
II	Data for the halved artery.	26
III	Theoretical data for halved and un-halved artery. The transverse cut did not significantly change the moment or curvature. . .	31

LIST OF FIGURES

FIGURE	Page
1	Bottom view of the artery. 8
2	Side view of the artery. The artery was approximately 50.23 mm long. 8
3	Align the artery in the jig such that a small portion overlaps the front edge 9
4	Tighten the jig by gently pushing the lower half of the jig upwards. Pinch the artery shut, but not tight enough to puncture the artery. 10
5	Puncture through one side of the artery with a needle, such that the tip slightly punctures through the lumen. Repeat for all 8 holes. 10
6	With forceps and tweezers, gently force each needle through the other half of the artery. 11
7	A side view after all needles are pushed through the artery. 11
8	Pull on suture at tip of needle until a small loop forms. Thread 2 4 inch strings halfway through loop. 12
9	Pull needle out and leave a small loop beneath the artery. Do not pull the strings all the way out. 12
10	Picture after all the needles have been pulled out with forceps. 13
11	Picture of artery ready to be attached to the apparatus. 14
12	Starting configuration of the experiment. 16
13	Image in Matlab after all points have been selected. 17

FIGURE	Page
14	Depiction of radially cut artery in cylindrical coordinates and outward normal vector. The outward unit normal of cut edge is (a), the radial axis (b), and the circumferential axis(c)The z-axis is coming out of the page. 20
15	Experimental moment vs curvature relationship of the un-halved artery. 28
16	Experimental moment vs curvature relationship of the halved artery. 28
17	Sum of the circumferential force \times thickness in the un-halved artery. Notice the sum is nearly null, which is expected since the artery is traction-free. 29
18	Theoretical moment vs curvature relationship of the un-halved artery. 29
19	Sum of the circumferential force \times thickness in the halved artery. Notice the sum is nearly null, which is expected since the artery is traction-free. 30
20	Theoretical moment vs curvature relationship of the halved artery. 30
21	Un-halved artery at 0° 38
22	Un-halved artery at 60° 38
23	Un-halved artery at 120° 39
24	Un-halved artery at 180° 39
25	Un-halved artery at 240° 39
26	Un-halved artery at 300° 39
27	Un-halved artery at 360° 40
28	Un-halved artery at 420° 40
29	Un-halved artery at 480° 40
30	Un-halved artery at 540° 40

FIGURE	Page
31	Un-halved artery at 600 ° 41
32	Un-halved artery at 660 ° 41
33	Halved artery at 0 ° 41
34	Halved artery at 60 ° 41
35	Halved artery at 120 ° 42
36	Halved artery at 180 ° 42
37	Halved artery at 240 ° 42
38	Halved artery at 300 ° 42
39	Halved artery at 360 ° 43
40	Halved artery at 420 ° 43
41	Halved artery at 480 ° 43
42	Halved artery at 540 ° 44
43	Halved artery at 600 ° 44
44	Halved artery at 660 ° 44
45	Halved artery at reference configuration ° 44

CHAPTER I

INTRODUCTION

All arteries possess some pre-stress. Even from the early stages of development as a fetus, arteries are continually deforming, growing, and adapting. However, to account for the growth and adaptation is beyond the scope of this work. Hence, it is assumed the artery is obtained in a given state, with a particular amount of pre-stress. A radial cut in a segmented artery with no external loads is referred to as the traction-free state. The traction-free state of tissues provides meaningful information which enables a better understanding of the growth and remodeling of vascular systems at the tissue level. For arteries, the opening angle or curvature of a radially cut artery enables the pre-stresses in the traction-free state to be calculated. The goals of this experiment are to 1. apply a pure moment to a radially cut ovine artery, 2. calculate the curvature of the artery segment opposite the cut, and 3. calculate the correlated pre-stresses. The pre-stresses are calculated using a Fung type model, and the pre-stresses are used to approximate the moments. Plots of global moment versus curvature are depicted to show the relationship for this experiment and for a Fung type model. The arteries will be tested in a passive saline solution.

A. Specific Aims

Specific Aim 1: Obtain publishable results on the curvature and pre-stresses of a traction-free state ovine artery. A designed apparatus capable of creating only a pure moment will be used to test the suspended artery. The radially cut artery will

The journal model is the Journal of Biomechanical Engineering.

be loaded until they achieve a ring configuration (when the artery appears to be intact). The device enables the angle of twist to be recorded. The angle of twist allows one to solve for the moment. With the moment known, we can solve for the pre-stress in the circumferential direction.

Problem with Aim 1: The experiment will employ only one radial cut; hence the traction-free state is not truly stress free. Studies have shown that radial cuts followed by circumferential cuts release more residual stress [1, 2].

Specific Aim 2: Create publishable figures for the moment versus curvature of the tested arteries and compare the calculated stresses with data using a Fung model.

CHAPTER II

BACKGROUND

Residual stress is the stress left in an artery when all external forces are removed. The zero-stress state is achieved when all residual stresses are relieved via a radial and/or circumferential cut(s). It has been shown [3, 4, 5, 6] that the zero-state stresses strongly relate to the homeostatic stress distributions in arteries. Chuong and Fung [3] proposed the study of residual stresses as an indicator of vascular remodeling. They believed the changes in the zero-stress state of arteries may be a useful way to better understand the growth and remodeling of arteries [3].

For arteries, transverse cuts relieve longitudinal stress, and then a radial cut releases circumferential stress, bending moment, and transverse shear at the cut section[7]. In a study of the zero-stress state Fung and Liu [8] concluded that the opening angle varies greatly along the aorta, and a single cut of a short segment yields a unique zero-stress configuration. However, other experimentalists [9, 10] suggested that multiple cuts were needed to achieve the stress-free state. To better understand the need for multiple or single cuts to achieve a stress-free state, [4] studied the residual stresses of arteries in several configurations neglecting smooth muscle tone. The configurations were 1) an unloaded intact artery, 2) an artery after a single transmural cut, and 3) the inner and outer rings of an artery created by combined radial and circumferential cuts. They found that the opening angle depends strongly on the material properties of the constituents in an artery and noticed several cuts may be needed to reach the zero-stress state.

The main tool to find the residual stresses is the opening angle. The opening angle

can be defined as the angle subtended at the midpoint of the inner circumference by its two ends[3]. However, in a recent study Criscione et al. [2] observed the curvature across from a radial cut may be a better tool to find residual stress. They claim the opening angle is a property of the entire cut artery with all of its circumferential and radial heterogeneities while the curvature opposite the cut has properties without the edge effects, meaning the radial segments in the region opposite the cut remain straight [2]. The proposed experiment will use the curvature across from a radially cut artery to calculate the pre-stresses and moment applied to the artery. The calculations will be made assuming the artery is a fung elastic and the calculated global moment versus curvature will be compared to the experimental relation of global moment versus curvature.

Fung postulated his model after an experiment in 1967. Aware of the non-linear stress-strain relation in soft tissues, Fung decided to plot stiffness versus stress in search of an explaining the non-linear relation [1]. Plotting stiffness versus stress showed a linear relation, and led to a first order ordinary differential equation (ODE). The solution to this ODE gave rise to an exponential relation of stress and strain. However, the conclusion of an exponential relation was based on an experiment solely on uniaxial extension, and not on three-dimensional data, which is ideal since soft tissues are anisotropic [1]. In good faith, Fung proposed his exponential as a three dimensional stress-strain relation, and is highly used today. It should be noted that there are serious problems with the Fung model. The model is a function of the principal invariants. Criscione [11] has shown the principal invariants are highly co-variant, hence, proving they are not a wise choice as a basis. Also, Walton [12] has shown the Fung model to be unstable unless all coefficients are unity.

To the best of my knowledge, there has not been a relation for moment versus curvature in the literature. However, Yu and Fung [13] conducted a bending experiment to try to find the load-deflection relationship by assuming the arteries (pig aortas) could be modeled as a simple beam with a force acting in the horizontal direction perpendicular to the beam. The experiment enforced three point bending to the artery, two ends were fixed and a suspended wire between the fixtures created the force. They found the neutral axis of the arteries to be one-third of the wall thickness from the endothelial. and the stress-strain relation was fit well by a linear correlation [13]. Xie and Fung [14] conducted another bending experiment on aortic strips from rats. They treated the artery as a curved beam, clamped at one end and free at the other. The free end was attached to a suspended wire and the deflection was measured. They, again, found the stress-strain correlation best fit by a linear model, and that large errors in the values of residual strain (up to 50 percent) occur when the wall is treated as homogeneous [14].

In conducting the experiment, it is important to control the environmental settings such as temperature and the physiological salt solution. Due to its viscoelastic properties, when an artery is cut, it springs open rapidly and continues to open slowly until reaching a constant angle after 20-30 minutes [15, 16]. Therefore, all measurements should be made after this time interval. Also, the effect of temperature needs to be monitored. Liu and Fung [7] observed no significant change of residual strain in the range of 25-40° Celsius. However, [17] confirmed the result but in the range of 10-37 ° Celsius. For this experiment, the physiological salt solution will be held at room temperature (20-25 ° C). In the literature, many experiments on residual stress used different solutions. Hence, there is not a solution

agreed upon in the field. Therefore, a phosphate buffered calcium and magnesium free saline solution will be used for the proposed experiment.

CHAPTER III

MATERIALS AND METHODS

A. Physiological Salt Solution

A phosphate buffered calcium and magnesium free saline solution was used to keep the artery passive. 500 mL were used to bathe the artery.

B. Equipment

Dr. Criscione has built an apparatus that applies a pure moment to an artery or any soft tissue attached to the torque transducer. The device suspends a thin cylindrical steel wire into a bath filled with a physiological salt solution. An artery is tied to the torque transducer so that any moment applied to the wire is also applied to the artery. The angle of twist was recorded.

A Sony digital camera was used with IC Capture(imaging software) to photograph the arteries prior to and during the experiment.

A jig built by Dr. Criscione and myself was used to symmetrically suture the artery.

C. Artery Preparation

The artery was donated by the College of Veterinary Medicine at Texas A&M University. The artery was handled following Texas A&Ms Laboratory Practices. It was stored at 5-10 ° Celsius and tested at room temperature (20-25°C). The specimen was an ovine thoracic artery.

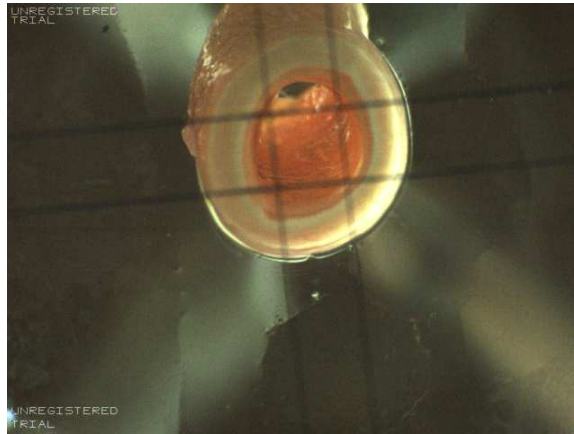


Fig. 1. Bottom view of the artery.

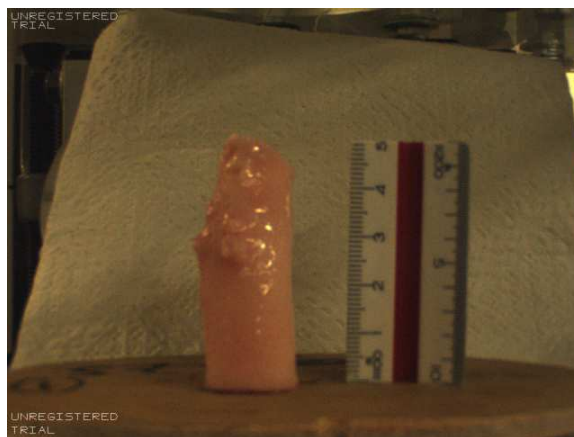


Fig. 2. Side view of the artery. The artery was approximately 50.23 mm long.

Before cutting the arteries, a picture was taken of the bottom and side view of the artery (Fig 1 and 2, respectively). The artery was cut to a length of approximately 50.23 mm using a sharp blade. Blunt dissection of the artery was done using forceps/tweezers to remove fat and connective tissues. The artery was kept moist during dissection.

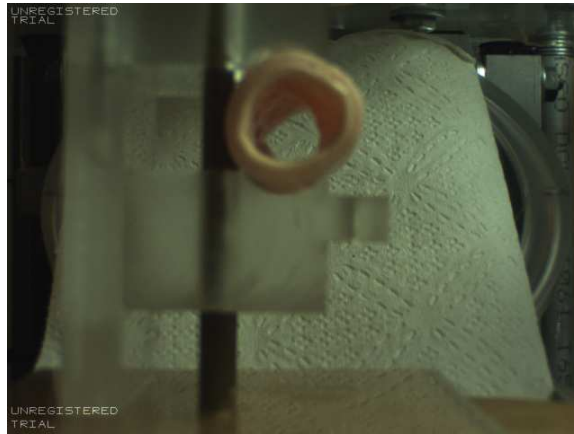


Fig. 3. Align the artery in the jig such that a small portion overlaps the front edge

D. Procedure

First, the artery is aligned in the jig (Fig 3). The jig is tightened so the artery can't move around, but not tight enough that the edge of the jig will puncture the artery (Fig 4). 8 regular sewing needles and a 5 inch string of suture (.5mm diameter) were threaded through each needle. Using forceps and tweezers, the needles were then inserted into the 8 holes beneath the artery (Fig 5). The needles were carefully pushed through the artery, one at a time, until the tip of the needle emerged out of the adventitia (Fig 6). On each artery, the tweezers and forceps were used to pull on the suture at the tip of the needle. The suture should be pulled until a small loop forms (Fig 8). 2 5 inch strings were threaded halfway through the loop, and then the needle was pulled with the forceps (Fig 9). After pulling all the needles out, the artery should appear as in Fig 10. The strings were pushed aside and the artery was cut length-wise with a sharp blade on the right side of the needles, with respect to Figure 7.



Fig. 4. Tighten the jig by gently pushing the lower half of the jig upwards. Pinch the artery shut, but not tight enough to puncture the artery.

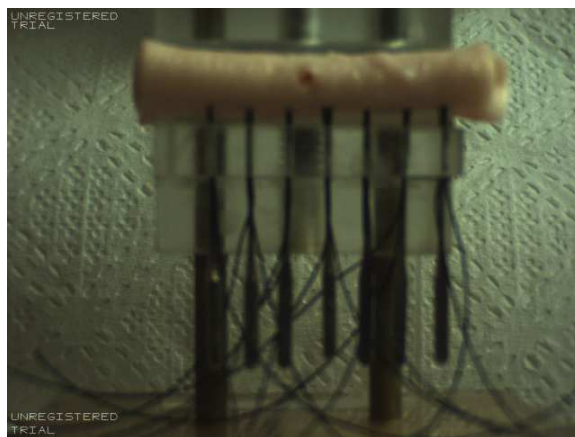


Fig. 5. Puncture through one side of the artery with a needle, such that the tip slightly punctures through the lumen. Repeat for all 8 holes.

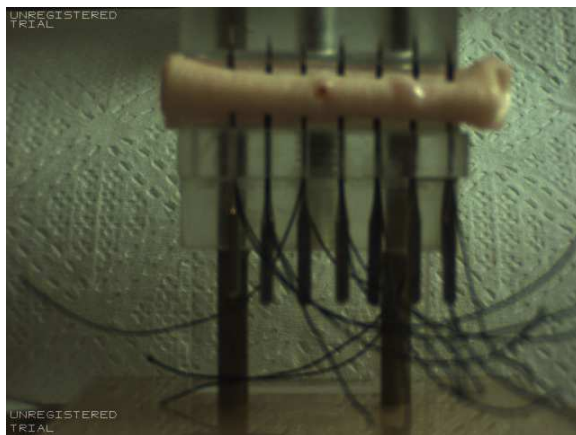


Fig. 6. With forceps and tweezers, gently force each needle through the other half of the artery.

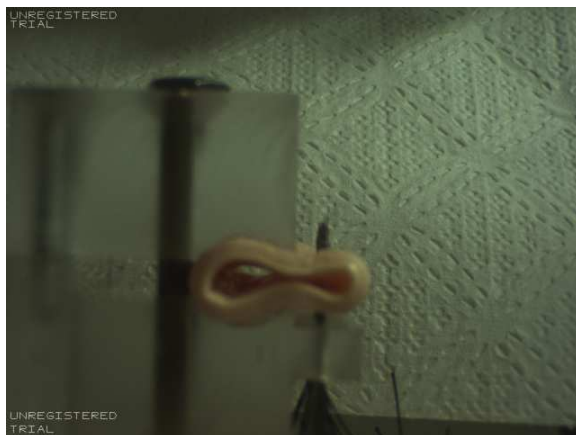


Fig. 7. A side view after all needles are pushed through the artery.

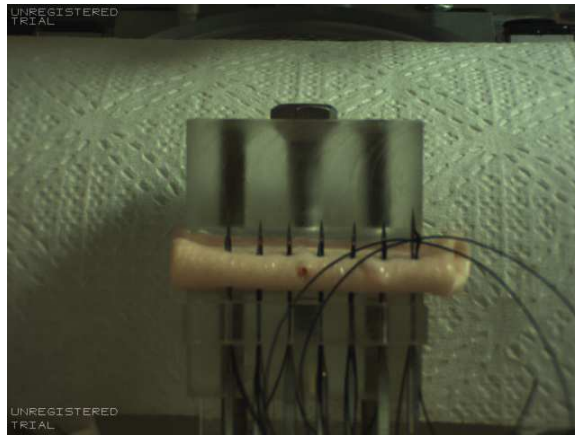


Fig. 8. Pull on suture at tip of needle until a small loop forms. Thread 2 4 inch strings halfway through loop.

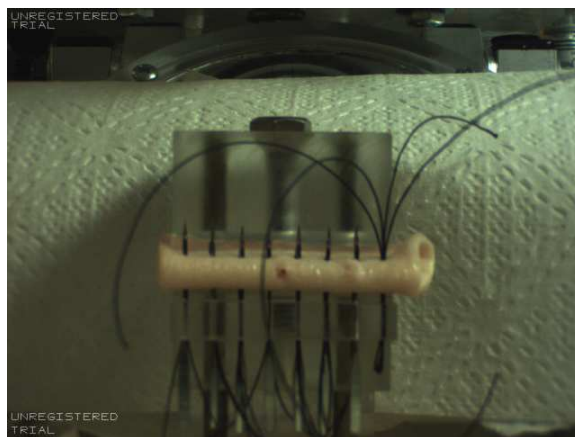


Fig. 9. Pull needle out and leave a small loop beneath the artery. Do not pull the strings all the way out.

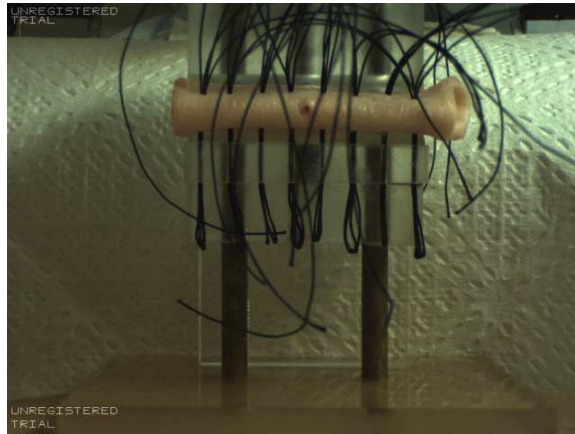


Fig. 10. Picture after all the needles have been pulled out with forceps.

When the artery is taken out of the jig, one side of the adventitia will have four string ends coming out and the opposite side of the adventitia will have two loops. Two ends of the same string were pulled through its corresponding hole so that the loop is now on the lumen side and the other loop remains outside the adventitia, as in Figure 9. Repeat this for all 8 holes. When done, the artery should open up like a rectangle with 8 loops in the lumen and 8 loops outside the adventitia. For every other loop on the lumen side, the loop was dismantled by pulling one end of the loop through the hole. Next, the string was threaded into the loop and the loop was pulled through. This was repeated for the other 3 sets of loops and strings on the lumen side. For the other side, the loops needed to be on the lumen side. This was achieved by threading a 5 inch string of suture through every other loop. The loops with the sting were pulled through to create a loop on the lumen side. From here, the same steps were repeated as the other side. The end result can be seen in Fig 11.

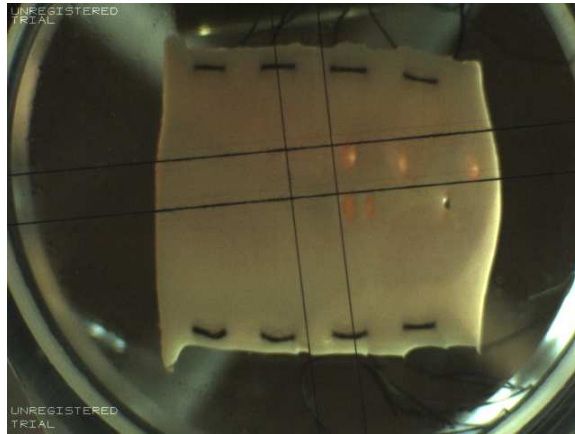


Fig. 11. Picture of artery ready to be attached to the apparatus.

The apparatus was aligned on a flat smooth surface, such that the suspended wire hung perpendicular to the ground.

The fixed brass block was unscrewed from the apparatus and the 8 holes on the fixed block were aligned with the 8 strings of the artery. The brass block was placed so the adventitia of the artery was adjacent to the side with countersunk holes. The artery was secured to the brass block with surgeon knots.

In the experiment, 3 steel reference pins (7mm long) were inserted transmurally at the bottom of the artery. The reference pins allowed the same points to be analyzed for curvature and θ_c calculations. Using forceps and tweezers, the pins were pushed through the artery when it was upright. This was made easier by standing the brass block up once the artery is attached. The pins were assured to be approximately the same height by placing the pins in the same thread of the forceps when placing them through the artery.

The brass block, with the artery sewn to it, was re-attached to the apparatus. The 8 pieces of suture were aligned into the corresponding 8 holes on the torque block hanging from the suspended wire, and surgeon knots were tied to secure the artery to the torque block. Once completed, the artery was bathed in 500 mL of physiological salt solution.

The top of the apparatus has a knob with 24 etchings. The etchings represent a $15 \pm 1.5^\circ$ change in angle. Once connected, the knob was turned clockwise to open the artery. The artery was opened until the torque block and brass block were almost touching (See Fig 12). This was the starting point of the experiment and denoted as a configuration of zero degrees. The zero angle was marked with a string taped to the etching, signifying the zero degree angle. Before starting the experiment, the number of turns of the knob was counted to identify the required twist to close the artery. Since the artery was thick, a picture was taken every 60° for analysis (every four turns of the knob). The procedure was done twice, once for the artery un-halved and when the artery was cut in half (from transverse cut). The angles ranged from -60° to 660° . It went to -60° after the artery was cut in half and the knob was turned back passed the initial position.

All data analysis was done using Matlab. Programs were written to analyze the photos and conduct numerical analysis. The code's explanations are below.

The code entitled 'intact' was written to solve for the intact inner and outer radius. The code brings up the image of the intact artery and asks the user to choose three points on the artery, with the second point being the middle point. From these three points, the code creates a circle and calculates, after scaling from the magnifica-

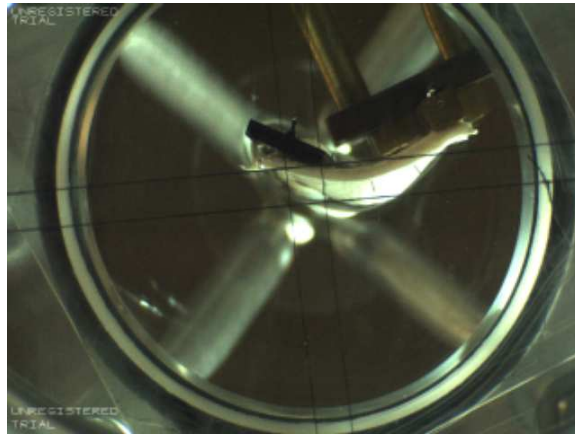


Fig. 12. Starting configuration of the experiment.

tion factor, the radius and center of that circle based on the 3 points. However, the intact radius was not used in the experiment but the inner and outer intact radius were found to be approximately $6.14 \pm .62$ mm and $8.48 \pm .62$ mm, respectively.

The code entitled 'thick' was used to calculate the thickness of the artery. The code brings up the image of the artery and asks the user to choose 4 points on the artery. The goal is to create two vectors, one representing the inner radius and one the outer radius. The starting point of the vectors are indifferent, however, both vectors need to share the same starting point. The other two points should be placed on the inner and outer edge of the artery. The magnitudes of the vectors are calculated and the difference multiplied by the scaling factor equates the thickness. The thickness was calculated on the artery opposite the cut when it was cut free and traction-free. Thickness was found to be 0.24 ± 0.1 mm.

The code entitled 'fung stress and JCCfung' use the method explained in chapter V to calculate for the pre-stresses. The codes were used to check the sum of the

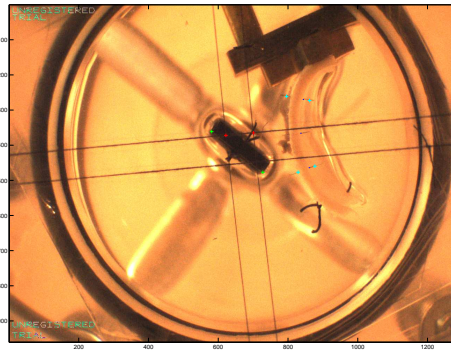


Fig. 13. Image in Matlab after all points have been selected.

circumferential stresses were approximately zero and that the radial stresses were almost null at the inner and outer radius, which is expected since the artery is traction free.

The code entitled 'image analysis' was used to analyze the experiment, and to calculate the curvature, θ_c , and the top and bottom angle of the torque block. The code first asks to input (in degrees) the angle which the top is being displaced. It then asks for 2 reference points, followed by two points on the torque block. The points are made to vectors and then the angle of the torque block is calculated with respect to the reference vector. The reference pins in the artery are then used to calculate the angle between the pins. The code asks for four points, two on each pin, to create vectors so that a subroutine in Matlab can calculate the angle between the pin vectors. Fig 13 depicts the image in Matlab after all the points have been selected. The radius of the artery in the configuration is found using code that is similar to that of the code 'intact'. The curvature is calculated by the relationship $1/r$.

CHAPTER IV

CONSTITUTIVE ASSUMPTIONS AND KINEMATICS

Let \mathbf{X} denote a material point on the artery opposite the radial cut in the traction-free reference configuration. Let \mathbf{x} denote a material point on the artery opposite the radial cut in the current configuration. By a motion, let χ be a one-to-one mapping that assigns to each \mathbf{X} a point \mathbf{x} in euclidean space:

$$\mathbf{x} = \chi(\mathbf{X}, t). \quad (4.1)$$

The deformation gradient (\mathbf{F}), right Cauchy-Green tensor (\mathbf{C}), and Green-St. Venant strain tensor (\mathbf{E}) are defined as:

$$\mathbf{F} = \frac{\partial \chi}{\partial \mathbf{X}}, \quad (4.2)$$

$$\mathbf{C} = \mathbf{F}^T \mathbf{F}, \quad (4.3)$$

$$\mathbf{E} = \frac{1}{2}(\mathbf{C} - \mathbf{I}). \quad (4.4)$$

, respectively, where the superscript T denotes the transpose of the linear transformation. A Fung-type stored energy function was assumed to characterize the response of the passive ovine artery. Fung proposed the function in 1979 to better fit the data, in lieu of a polynomial stored energy function, for iliacs, carotids, thoracic and abdominal aortas in rabbit arteries. Fung's stored energy function is defined as:

$$W = \frac{1}{2}c(e^Q - 1). \quad (4.5)$$

where Q is defined as:

$$\begin{aligned}
 Q = & c_1 E_{RR}^2 + c_2 E_{\theta\theta}^2 + c_3 E_{ZZ}^2 + 2c_4 (E_{RR} E_{\theta\theta}) + 2c_5 (E_{\theta\theta} E_{ZZ}) + 2c_6 E_{ZZ} E_{RR} \\
 & + c_7 (E_{R\theta}^2 + E_{\theta R}^2) + c_8 (E_{\theta Z}^2 + E_{Z\theta}^2) + c_9 (E_{ZR}^2 + E_{RZ}^2).
 \end{aligned} \tag{4.6}$$

where c_i are material parameters. For this model of our experiment, the material constants are taken from values published by Chuong and Fung [3] and are: $c = 22.4kPa$, $c_1 = 0.0499$, $c_2 = 1.0672$, $c_3 = 0.4775$, $c_4 = 0.0042$, $c_5 = 0.0903$, $c_6 = 0.0585$. The axial strain, E_{ZZ} is assumed unity, hence $\lambda_z = 1$, and the E_{ZZ} component of the Green-Strain is zero. Therefore, c_7 , c_8 , and c_9 are not needed. By the same argument, c_3 , c_5 , and c_6 are extraneous.

For this problem, the artery is assumed to be hyperelastic, homogeneous, incompressible, and anisotropic. The residual stresses were calculated using a Cauchy stress relation prescribed as:

$$\mathbf{T} = -p\mathbf{I} + \mathbf{F} \frac{\partial \mathbf{W}}{\partial \mathbf{E}} \mathbf{F}^T \tag{4.7}$$

where p is the Lagrange multiplier that enforces the constraint of incompressibility, and \mathbf{I} is the identity. Since the deformation will only contain diagonal terms, the Cauchy stress relation can be written as:

$$\mathbf{T} = -p\mathbf{I} + \mathbf{F}^2 \frac{\partial \mathbf{W}}{\partial \mathbf{E}} \tag{4.8}$$

CHAPTER V

MODELING THE EXPERIMENT

The first part of the experiment is to theoretically model and calculate the radial and circumferential pre-stresses in an artery; beginning when the radially cut artery is in a traction-free reference configuration and ending when the artery is closed to a ring configuration. The model employs a semi-inverse approach to solve for the radial and circumferential pre-stresses using a cylindrical coordinate system to seek a mapping $(R, \Theta, Z) \mapsto (r, \theta, z)$ such that the artery undergoes the motion:

$$\begin{aligned} r &= r(R), \\ \theta &= \frac{\theta_c \Theta}{\Theta_o}, \\ z &= \Lambda Z, \end{aligned} \tag{5.1}$$

where θ_c is the angle in the configuration, and $\Lambda = 1$. Figure 14 depicts the orientation of the cut artery. The outward unit normal is 'a', the radial axis is 'b', the circumferential axis is 'c' and the z axis is out of the page. The artery will be considered to be axis-symmetric and have the following configuration:

For this mapping in cylindrical coordinates the deformation gradient is:

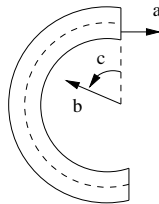


Fig. 14. Depiction of radially cut artery in cylindrical coordinates and outward normal vector. The outward unit normal of cut edge is (a), the radial axis (b), and the circumferential axis (c). The z-axis is coming out of the page.

$$[\mathbf{F}] = \begin{bmatrix} \frac{\partial r}{\partial R} & 0 & 0 \\ 0 & \frac{\theta_c r}{\Theta_o R} & 0 \\ 0 & 0 & 1 \end{bmatrix} \quad (5.2)$$

From the incompressibility assumption,

$$\det[\mathbf{F}] = 1 \quad (5.3)$$

and

$$\frac{\partial r}{\partial R} = \frac{\Theta_o R}{\theta_c r} \quad (5.4)$$

The reference volume is

$$Vol_{ref} = (R_o^2 - R_i^2)\Theta_o L, \quad (5.5)$$

and the current volume is

$$Vol_{cur} = (r_o^2 - r_i^2)\theta_c L, \quad (5.6)$$

where r_o is obtained by setting the volume of the artery in the reference equal to the volume in the current configuration.

$$r_o = \frac{\sqrt{\theta_c(\theta_c r_i^2 + \Theta_o R_o^2 - \Theta_o R_i^2)}}{\theta_c} \quad (5.7)$$

Measuring R_o , R_i , and r_i will allow r_o to be calculated.

The right Cauchy-Green stretch tensor and Green strain tensor have the following representations:

$$[\mathbf{C}] = \begin{bmatrix} \left(\frac{\Theta_o R}{\theta_c r}\right)^2 & 0 & 0 \\ 0 & \left(\frac{\theta_c r}{\Theta_o R}\right)^2 & 0 \\ 0 & 0 & 1 \end{bmatrix}, \quad [\mathbf{E}] = \begin{bmatrix} \left(\frac{\Theta_o R}{\theta_c r}\right)^2 - 1 & 0 & 0 \\ 0 & \left(\frac{\theta_c r}{\Theta_o R}\right)^2 - 1 & 0 \\ 0 & 0 & 0 \end{bmatrix} \quad (5.8)$$

The equations for the radial and circumferential residual stresses take the form, respectively:

$$T_{rr} = -p + \left(\frac{\Theta_o R}{\theta_c r}\right)^2 \frac{\partial W}{\partial E_{RR}}, \quad T_{\theta\theta} = -p + \left(\frac{\theta_c r}{\Theta_o R}\right)^2 \frac{\partial W}{\partial E_{\Theta\Theta}} \quad (5.9)$$

The radial component of the equilibrium equation in cylindrical coordinates reduces to:

$$\frac{\partial T_{rr}}{\partial r} + \frac{T_{rr} - T_{\theta\theta}}{r} = 0 \quad (5.10)$$

Integrating equation (5.10) and remembering the artery is traction-free, shows the stress in the radial direction is:

$$T_{rr}(r) = \int_{r_i}^{r_o} (T_{\theta\theta} - T_{rr}) \frac{1}{r} dr \quad (5.11)$$

Now that $T_{rr}(r)$ is known, as well as $\frac{\partial W}{\partial E_{RR}}$ and $\left(\frac{\Theta_o R}{\theta_c r}\right)^2$, the Lagrange multiplier can be solved. The Lagrange multiplier takes the form:

$$p(r) = \left(\frac{\Theta_o R}{\theta_c r}\right)^2 \frac{\partial W}{\partial E_{RR}} - T_{rr}(r) \quad (5.12)$$

With the Lagrange multiplier known, it is now possible to solve for the residual stresses. The code titled Fung Stress in the Appendix followed this method to solve for the radial and circumferential residual stresses. Once the residual stresses are calculated, the next step is to calculate for the moment. The traction vector is the

stress transposed operating on the outward unit normal.

$$\mathbf{t} = \mathbf{T}^T \mathbf{n} \quad (5.13)$$

In my case, the traction takes the form

$$\mathbf{t} = \begin{bmatrix} T_{rr} & T_{r\theta} & T_{rz} \\ T_{\theta r} & T_{\theta\theta} & T_{\theta z} \\ T_{zr} & T_{z\theta} & T_{zz} \end{bmatrix} \begin{bmatrix} 0 \\ -e_\theta \\ 0 \end{bmatrix} = - \begin{bmatrix} T_{r\theta} \\ T_{\theta\theta} \\ T_{z\theta} \end{bmatrix} \quad (5.14)$$

Since the experiment is traction-free, it implies

$$\int T_{r\theta} da = 0, \int T_{\theta\theta} da = 0, \int T_{z\theta} da = 0 \quad (5.15)$$

The sum of the moments is zero since the the artery is in equilibrium, hence

$$\sum \mathbf{M} = \mathbf{M}_{edge} + \mathbf{M}_{applied} = 0 \quad (5.16)$$

From the general moment equation, we find \mathbf{M}_{edge} to be

$$\begin{aligned} \mathbf{M}_{edge} &= \int r \mathbf{e}_r \times \mathbf{t} da = \int r \mathbf{e}_r \times (-T_{r\theta}(r) \mathbf{e}_r - T_{\theta\theta}(r) \mathbf{e}_\theta - T_{z\theta}(r) \mathbf{e}_z) da \quad (5.17) \\ &= - \int \int r T_{\theta\theta}(r) dr dz \mathbf{e}_z + \int \int r T_{z\theta}(r) dr dz \mathbf{e}_\theta. \end{aligned}$$

Since the device is weighted by a torque transducer, the stress in the $T_{z\theta}$ will be assumed negligible and thus I have an equation that will correlate moment to circumferential residual stress, and, hence, by equation 5.16 the moment applied is

$$M_{applied} = L \int_{r_i}^{r_o} r T_{\theta\theta}(r) dr. \quad (5.18)$$

In the experiment, the angle of twist will be recorded. The moment is related

to the angle of twist by the general relation:

$$M = \kappa \Delta\theta, \quad (5.19)$$

where $\Delta\theta$ is the twist and is defined as

$$\Delta\theta = \theta_{top} - \theta_{bottom}, \quad (5.20)$$

and κ is the stiffness of the wire. The stiffness of the wire was found experimentally. The stiffness of the wire can be found by the correlation:

$$\omega = \sqrt{\frac{\kappa}{I_{zz}}} \quad (5.21)$$

where ω is the natural frequency and I_{zz} is the second moment of inertia about the z-axis. The equation for I_{zz} is

$$I_{zz} = m \frac{r^2}{2} \quad (5.22)$$

where m is the mass of the solid cylinder and r is the radius of the cylinder. I_{zz} was found simply by weighing the solid cylinder and the screw fixing the wire to the cylinder, and by measuring the radius of the cylinder. ω was found using IC capture. A video was created in order to count how many times a marker on the cylinder crossed a referential axis after a twist was applied to the cylinder. The number of times it crossed the referential axis was divided by 2 times the duration of the mini-experiment(in seconds). I_{zz} and κ were then plugged back into equation (5.19) to for the moment.

CHAPTER VI

RESULTS

All the results are from a single thoracic ovine artery. The intact artery had an inner and outer intact radius of $6.14 \pm .62$ mm and $8.48 \pm .62$ mm, respectively. The accuracy of measurements were found by analyzing the cut-free traction-free artery a total of six times. From this analysis, the standard deviation of the measured curvature is ± 0.001 1/mm, bottom angle $\pm .0088$ rad, top angle $\pm .026$ rad, $\theta \pm 0.99^\circ$, $\Delta\theta \pm .088$ rad, thickness $\pm .1$, and moment $\pm .025$ mN·mm.

Solving equations 5.21 and 5.22 yielded the values of κ to be 2.83 mN·mm, and I_{ZZ} to be 4.36353e-06, where $r=.0126$ m and $m=54.65$ g.

Table I is the data measured for the artery before the transverse cut. The first row contains the measured values for the artery when it was cut free and traction-free, and is denoted as the reference configuration. Hence, Θ_o is fixed constant at 30° in the calculations. The top and bottom angle are equal since the artery is cut free and there is no counter moment applied. The artery was cut free after the experiment was completed and the knob at the top of the apparatus was turned approximately 660° for the experiment. Note, the moment is zero in the reference configuration and should be zero again between 300 and 360° . The measurements at 300 and 360° are probably off due to human error.

Table II is the data measured for the artery after a transverse cut. The first row indicates all the values for the reference configuration; Θ_o was fixed at 31° for all calculations. The zero moment occurred between 240 and 300° .

Table I. Data for the un-halved artery.

Angle °	Curvature (1/m)	Top displacement (rad)	θ°	Bottom displacement (rad)	$\Delta\theta$ (rad)	Moment (mN·mm)
660	0.043	11.51	31	11.516	0	0
0	-0.042	0	52	2.364	-2.364	-6.69
60	-0.024	1.04	38	2.756	-1.708	-4.83
120	-0.019	2.09	26	3.388	-1.288	-3.65
180	0.016	3.14	7	4.408	-1.264	-3.57
240	0.030	4.18	19	4.764	-0.572	-1.62
300	0.023	5.23	22	5.124	0.108	0.31
360	0.053	6.28	41	5.556	0.732	2.07
420	0.079	7.33	61	6.026	1.308	3.70
480	0.098	8.37	71	6.572	1.808	5.11
540	0.123	9.42	87	7.056	2.364	6.70
600	0.148	10.47	76	7.624	2.848	8.06
660	0.171	11.51	65	8.224	3.288	9.32

Table II. Data for the halved artery.

Angle °	Curvature (1/m)	Top displacement (rad)	θ°	Bottom displacement (rad)	$\Delta\theta$ (rad)	Moment (mN·mm)
660	0.044	11.51	30	11.516	0	0
-60	-0.063	-1.04	66	2.064	-3.116	-8.82
0	-0.045	0	50	2.464	-2.464	-6.98
60	-0.030	1.04	37	3.016	-1.964	-5.57
120	0.001	2.09	3.	4.110	-2.016	-5.71
180	0.015	3.14	9	4.616	-1.472	-4.16
240	0.027	4.18	19	5.008	-0.816	-2.31
300	0.045	5.23	34	5.400	-0.164	-0.47
360	0.043	6.28	30	5.308	0.972	2.75
420	0.066	7.33	53	5.864	1.472	4.16
480	0.094	8.37	71	6.472	1.908	5.39
540	0.120	9.42	89	7.096	2.332	6.59
600	0.150	10.47	74	7.696	2.772	7.85
660	0.170	11.51	62	8.200	3.316	9.39

Table III has the calculated values for the curvature and moment of the artery. The input to the calculations were taken from the measured data. The reference and inner radius were found using the reciprocal of the reference and configuration curvature. Configuration curvature refers to the curvature at a specific angle (the

column) from table I and II. The outer reference and configuration radius were found using by adding the thickness of the artery in the cut-free, traction-free configuration to the reference and inner radius. The code "thick" found the thickness to be $2.4 \pm .1$ mm. The calculations for the theoretical model revealed to be equivalent (after accounting for significant figures) before and after the transverse cut. Note, the data had to be scaled in order for the moments to be on the same order. The c in fung's model was multiplied by 10 since the coefficients found by Chuong and Fung [3] were determined from data of a rabbit's thoracic aorta, a much smaller and thinner specimen.

Figs 15 and 16 depict the experimental data on the relationship between moment and curvature for the artery un-halved and halved, respectively. Figs 17 and 19, show the net circumferential stresses are approximately zero when the artery is un-halved and halved, respectively. Figs 18 and 20 show the calculated relationship for moment vs curvature. The calculated values did not yield the same moment as the experiment, but this is likely due to using constants that were found for a smaller artery.

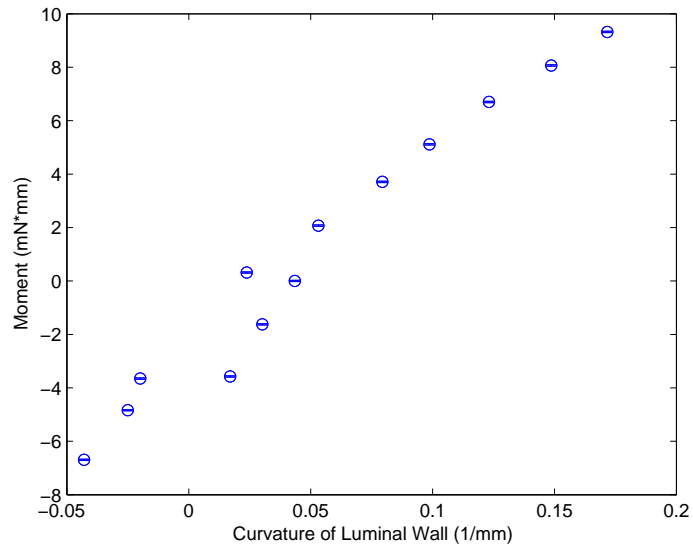


Fig. 15. Experimental moment vs curvature relationship of the un-halved artery.

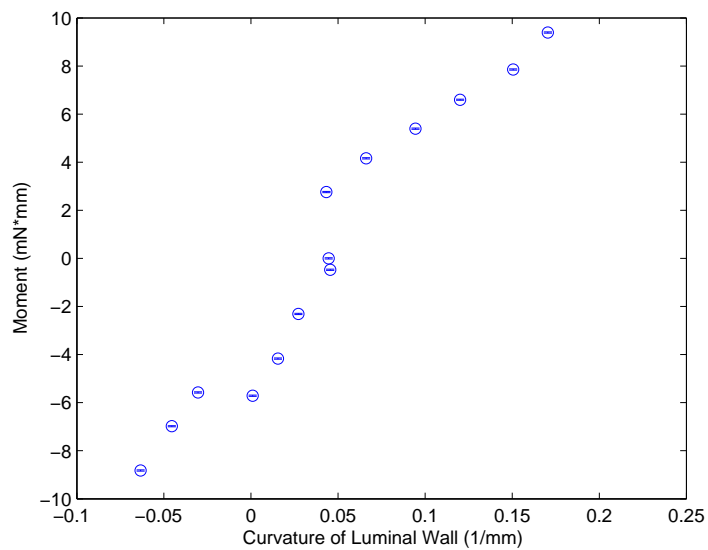


Fig. 16. Experimental moment vs curvature relationship of the halved artery.

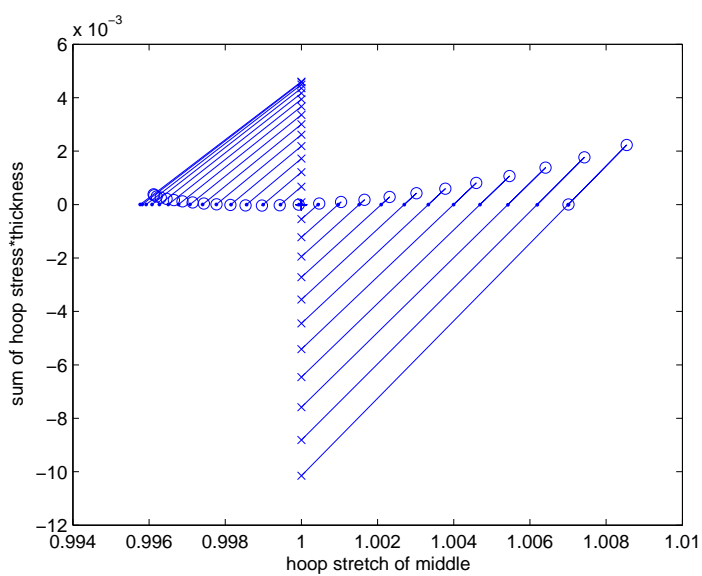


Fig. 17. Sum of the circumferential force \times thickness in the un-halved artery. Notice the sum is nearly null, which is expected since the artery is traction-free.

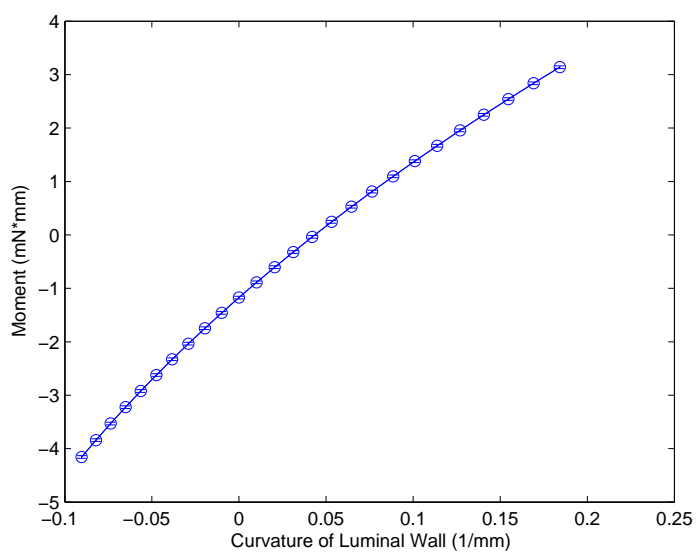


Fig. 18. Theoretical moment vs curvature relationship of the un-halved artery.

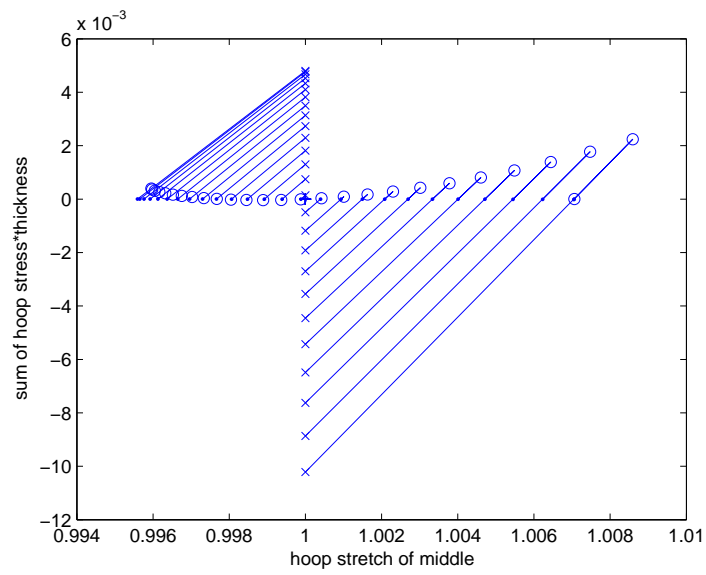


Fig. 19. Sum of the circumferential force \times thickness in the halved artery. Notice the sum is nearly null, which is expected since the artery is traction-free.

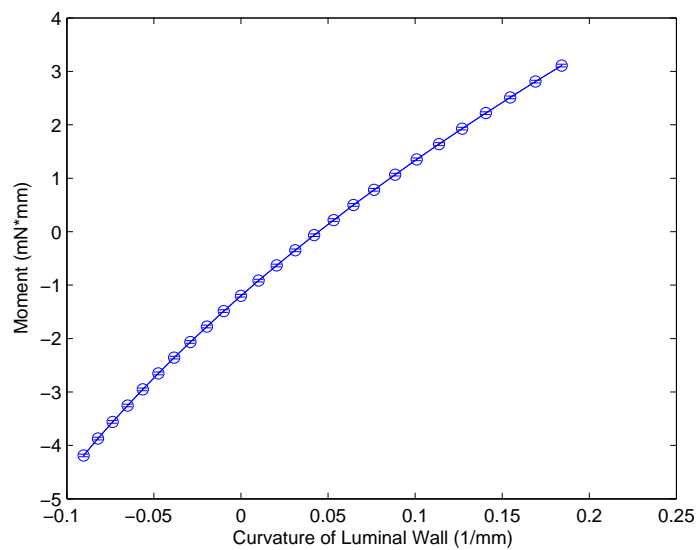


Fig. 20. Theoretical moment vs curvature relationship of the halved artery.

Table III. Theoretical data for halved and un-halved artery. The transverse cut did not significantly change the moment or curvature.

Curvature (1/mm)	Moment (mN· mm)
-.090	-4.25
-.082	-3.93
-.073	-3.61
-.065	-3.30
-.056	-2.99
-.047	-2.69
-.038	-2.39
-.029	-2.09
-.019	-1.80
-.099	-1.51
0	-1.22
.010	-.930
.020	-.642
.031	-.354
.042	-.067
.053	.220
.064	.507
.076	.795
.088	1.08
.100	1.37
.113	1.66
.126	1.95
.140	2.25
.154	2.55
.169	2.85
.184	3.15

CHAPTER VII

DISCUSSION AND CONCLUSION

The experimental moment versus curvature and the Fung moment versus curvature both displayed a linear relation to the applied deformation. Even after the transverse cut, the moment did not change significantly from configuration to configuration. In the Fung model, the moment versus curvature relation was the same before and after the cut. However, note that in the experimental data, after the transverse cut a rotation between 300 and 360° was needed to pass the zero moment while a rotation between 240 and 300° was needed to pass the zero moment when the artery was intact. This observation is counter intuitive, however, it is feasible that the transverse cut did not alleviate the axial load since the artery is sutured to two blocks, or it could be due to human error.

The transverse cut introduced new edges in the artery, however, edge effects did not influence the outcome. The moment remained the same before and after the transverse cut. Hence, the plane strain was the same before and after the cut, and the new edges introduced had the same effect as the initial edges.

A radial cut along the artery should relieve most of the circumferential stress. If completely relieved and no load is applied in the θ direction, then the sum of the stresses in the θ direction should equate to zero. Fig 17 and 19 show the sum of the stresses to be zero. The \times on the plot indicate where the circumferential stretch is unity. The o are the initial calculated points through the thickness at where the neutral axis is located and the \bullet is where the code converged as the neutral axis. The plots imply that the neutral axis is closer to the inner wall since the initial cal-

culated points are approximately the same as the neutral axis when in compression. The plots infer that the neutral axis is close to the calculated point when the artery is in compression and farther away when the artery is in tension. This idea supports Yu and Fung [13] whom found the neutral axis of the arteries to be one-third of the wall thickness from the endothelial. It is known that in physiological conditions, the lumen is in compression and the adventitia is in tension. Also, it is interesting to note that Fig 17 and 19 have relatively the same linear slope, indicating a linear stress-strain relation.

The artery was assumed to be hyperelastic, homogeneous, incompressible, and isotropic for the experiment. It is important to realize these assumptions are not realistic, but are used to simplify the problem, and to get initial data. It is well known that the artery is inhomogeneous. The three distinct layers known are the intima, media, and adventitia. The hyperelastic assumption assumes the stress can be derived from a potential. However, the potential being used is postulated and not actually derived, hence the uniqueness is hard to verify. In general, soft tissues are anisotropic, displaying different material responses along different fiber directions when subject to a perturbation. Better assumption will be made once material laws are discovered for different types of soft tissues, but until then, these types of assumption aid to gain insight on the mechanical properties of soft tissues.

This experiment has potential to be expanded upon. In this study, the artery was held fixed at an axial stretch of unity. It would be interesting to make adjustments to the apparatus so axial stretch can be incorporated into the experiment. It would be ideal to conduct the experiment at an axial stretch closer to a physiological parameter, such as an axial stretch of 1.6. Also, this experiment dealt with relatively

small strains. If possible, it would be interesting to apply bigger strains, and see if the global moment versus curvature is non-linear. Lastly, in order to see a trend, more arteries need to be tested to validate the linear trend observed.

In conclusion, the Fung model yielded a linear global moment versus curvature relationship, as well as the global moment versus curvature relationship for the experiment. Despite both small and large stretches, the strains felt by the artery were not influential enough to display a non-linear correlation for moment vs curvature. These results support [13, 14] in which they observed that linear constitutive equations govern the mechanical properties of the vessel wall in the small strain region.

REFERENCES

- [1] Humphrey, J., 2002, *Cardiovascular Solid Mechanics: Cells, Tissues, and Organs*, Springer-Verlag, New York.
- [2] Criscione, J.C., Omens, J.H., McCulloch, A.D., 2003, "Complex distributions of residual stress and strain in the mouse left ventricle: experimental and theoretical models," *Biomechan Model Mechanobiol.*, **1**, pp. 267-277.
- [3] Chuong, C.J., Fung, Y.C., 1986, "On residual stresses in arteries," *J. Biomech.*, **108**, pp. 189-192.
- [4] Humphrey, J., Taber L., 2001, "Stress-modulated growth, residual stress, and vascular heterogeneity," *J. Biomech Eng.*, **123**, pp. 528-535.
- [5] Zeller, P.J., Skalak, T.C., 1998, "Contribution of individual structural components in determining the zero-stress state in small arteries," *J. Vasc. Res.* **35**, pp. 8-17.
- [6] Peterson, S.J., Okamoto R.J., 2000, "Effect of residual stress and heterogeneity on circumferential stress in the arterial wall," *J. Biomech. Eng.*, **122**, pp. 454-456.
- [7] Fung, Y.C., Liu S.Q., 1992, "Strain distribution in small blood vessels with zero-stress state taken into consideration," *Am. J. Physiol.*, **262**, pp. H544-H552.
- [8] Fung, Y.C., Liu, S.Q., 1989, "Change of residual strains in arteries due to hypertrophy caused by aortic constriction," *Circ. Res.*, **65**, pp. 1340-1349.

- [9] Vaishnav, R.N., Vossoughi, J., 1987, "Residual stress and strain in aortic segments," **20**(3), pp. 235-239.
- [10] Greenwald, S.E., Moore, J.E. Jr, Rachev, A., Kane, T.P., Meister, J.J., 1997, "Experimental investigation of the distribution of residual strains in the artery wall," **119**(4), pp. 438-444.
- [11] Criscione, J.C., 2003, "Rivlins representation formula is ill-conceived for the determination of response functions via biaxial testing," *Journal of Elasticity*, **70**, pp. 129-147.
- [12] Wilber, J.P., Walton J.R., 2002, "The convexity properties of a class of constitutive models for biological soft tissues," *Mathematics and Mechanics of Solids*, **7**, pp. 217-235.
- [13] Yu, Q., Zhou, J., Fung, Y.C., 1993, "Neutral axis location in bending and Young's modulus of different layers of arterial wall," *Am. J. PHysiol., Heart and Circulatory Physiology*, **265**, pp. H52-H60.
- [14] Xie, J., Zhou, J., Fung, Y.C., 1995, "Bending of blood vessel wall: stress-strain laws of the intima-media and adventitial layers," *ASME Journal of Biomechanical Engineering*, **117**, pp. 136-145.
- [15] Rachev, A, Greenwald, S.E., 2003, "Residual strains in conduit arteries," *J. Biomech.*, **36**, pp. 661-670.
- [16] Rachev, A., 1997, "Theoretical study of the effect of stress-dependent remodeling on arterial geometry under hypertensive conditions," *J. Biomech.*, **30**, pp. 819-827.

- [17] Rachev, A., Hayashi, K., 1999, "Theoretical study of the effects of vascular smooth muscle contraction on strain and stress distributions in arteries," *Ann. Biomed. Eng.*, **27**, pp. 459-468.

APPENDIX A

PICTURES OF EXPERIMENT

The following pictures show the process of the experiment, starting from the zero degree configuration all the way to 660 degrees with 60 degree increments. The very last picture is the artery in the cut free traction-free state. The first several pictures are for the artery before the transverse cut. Once the pictures show the artery close, the next picture is when it is in the initial configuration after the transverse cut. Note the initial position after the transverse cut is at -60 degrees. The last picture is the reference configuration.

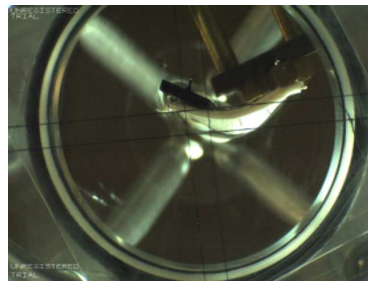


Fig. 21. Un-halved artery at 0 °.

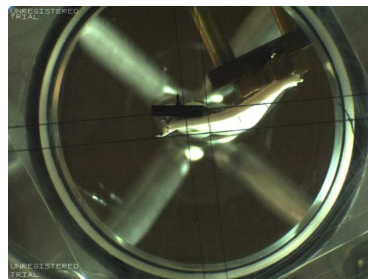


Fig. 22. Un-halved artery at 60 °.

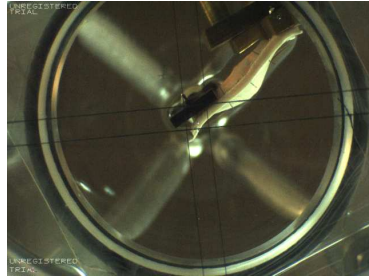


Fig. 23. Un-halved artery at 120 °.

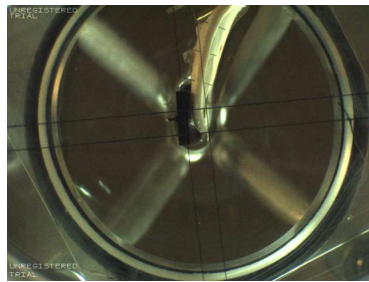


Fig. 24. Un-halved artery at 180 °.

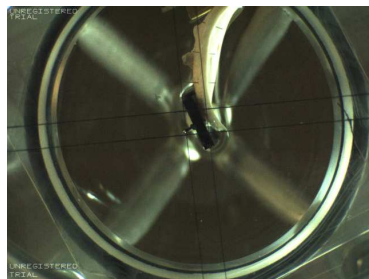


Fig. 25. Un-halved artery at 240 °.

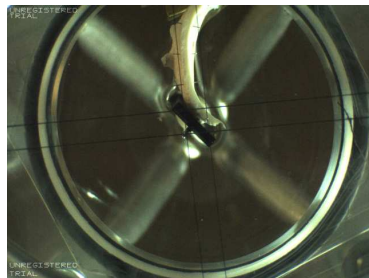


Fig. 26. Un-halved artery at 300 °.



Fig. 27. Un-halved artery at 360 °.



Fig. 28. Un-halved artery at 420 °.



Fig. 29. Un-halved artery at 480 °.



Fig. 30. Un-halved artery at 540 °.

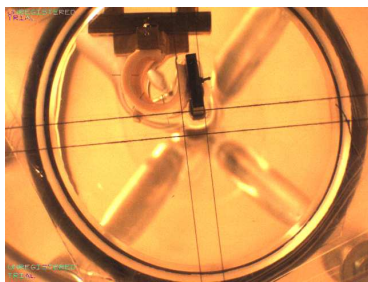


Fig. 31. Un-halved artery at 600 °.

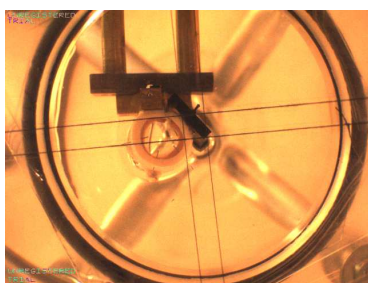


Fig. 32. Un-halved artery at 660 °.

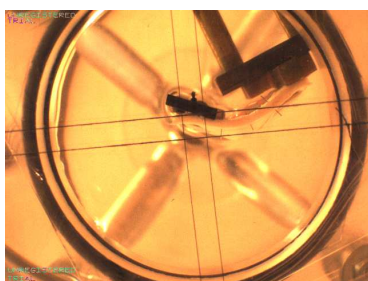


Fig. 33. Halved artery at 0 °.

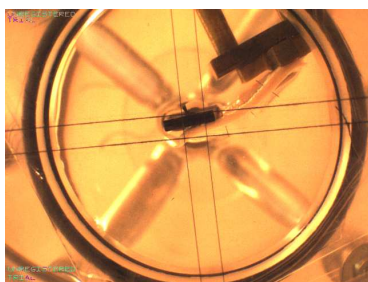


Fig. 34. Halved artery at 60 °.

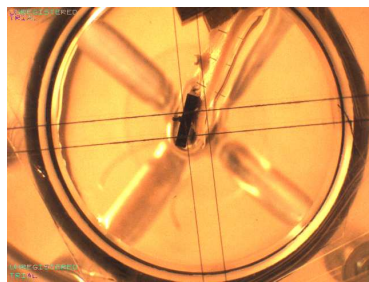


Fig. 35. Halved artery at 120 °.

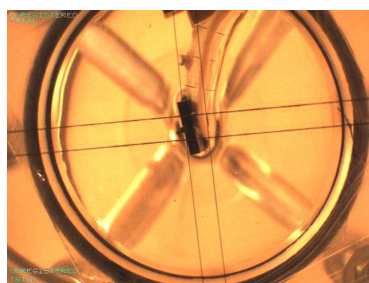


Fig. 36. Halved artery at 180 °.

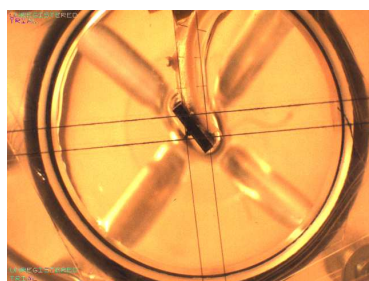


Fig. 37. Halved artery at 240 °.

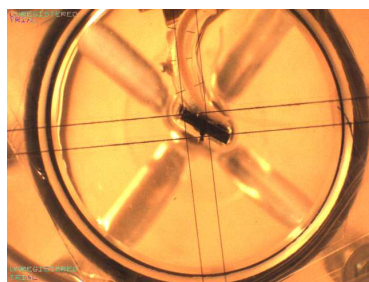


Fig. 38. Halved artery at 300 °.

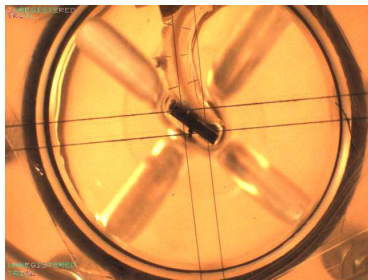


Fig. 39. Halved artery at 360 °.

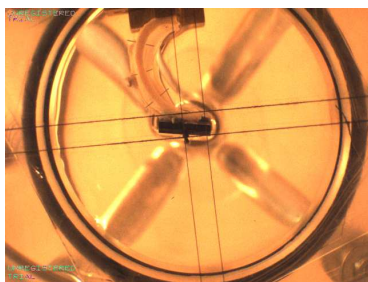


Fig. 40. Halved artery at 420 °.

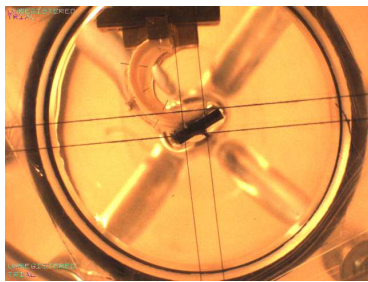


Fig. 41. Halved artery at 480 °.

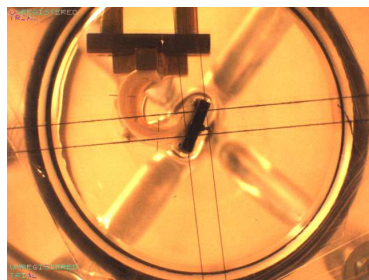


Fig. 42. Halved artery at 540 °.

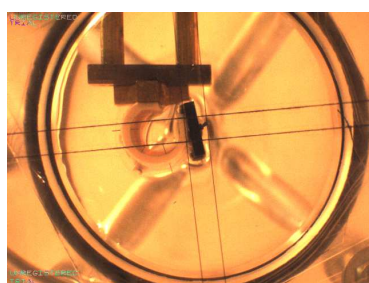


Fig. 43. Halved artery at 600 °.

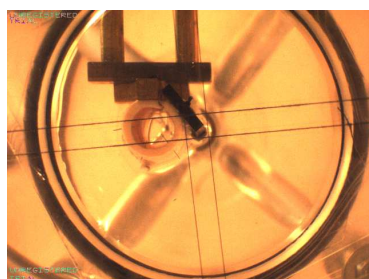


Fig. 44. Halved artery at 660 °.

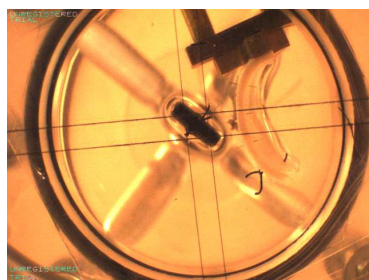


Fig. 45. Halved artery at reference configuration °.

APPENDIX B

CODES

```

<div class="moz-text-flowed" style="font-family: -moz-fixed">% function fung =
fungstress2(ri)

close all;
clear all;
clc;
syms rho ri ra
global r_nuet theta theta0 Ri Ra
%List of given constants
c = 22.4; % in kPa
c1= 0.0499;
c2= 1.0672;
c3= 0.4775;
c4= 0.0042;
c5= 0.0903;
c6= 0.0585;

%List of defined variables
% Ri=22.4215e-3; %in meters for cut artery
Ri = 22.9885e-3; %in meters for uncut artery
% ra=4.98e-3; %in meters
% Ra = 24.8215e-3; % in meters for cut artery
Ra = 25.3885e-3; % in meters for uncut artery
% ri=1.39e-3; %in meters
lambda=1;
theta = (114.6*pi/180);
theta0=30.9487*pi/180;
format long

% R = sqrt(theta0*(theta0*Ri^2 + theta*rho^2-theta*ri^2)) / theta0;
% Ra = subs(R,'rho',ra)

% rmid = (theta0*Ra) / theta;
TH = Ra - Ri
% r_mid = [rmid+.1*th rmid rmid-.1*th]

% r = sqrt(theta*(theta0*Ra^2 - theta0*Ri^2 + theta*ri^2)) / theta
ri = (1 / .1717)*1e-3 % in meters
ra = sqrt(theta*(theta0*Ra^2 - theta0*Ri^2 + theta*ri^2)) / theta
th = ra-ri
mid = (ra+ri)/2
r_mid = [mid+.1*th mid mid-.1*th]
for i= 1:length(r_mid)
ri(i) = sqrt(theta*(theta0*Ri^2 - theta0*Ra^2 + theta*r_mid(i)^2)) / theta;
end
% ri = eval(ri)

```

```

for i = 1:3
    ra(i) = sqrt(theta*(theta0*Ra^2 - theta0*Ri^2 + theta*r_mid(i)^2)) /
theta;
end
% ra = eval(ra)
for j = 1:3

% Using the given variables, the deformation gradient is calculated as
% follows:
% F = [(theta0*R)/(theta*rho) 0 0; 0 (theta*rho)/(theta0*R) 0; 0 0 1];
F11 = (theta0*Ra)/(theta*rho);
F22 = (theta*rho)/(theta0*Ra);
F33 = lambda;

% Green Strain
Err = 0.5*[F11^2- 1];
Ett = 0.5*[F22^2- 1];
Ezz = 0.5*[F33^2- 1];

Q = c1*(Err^2)+c2*(Ett^2)+c3*(Ezz^2)+2*c4*Err*Ett+2*c5*Ett*Ezz+2*c6*Ezz*Err;
% W = c*(exp(Q)-1);
dWrr = [c*(exp(Q)*(2*c1*Err+2*c4*Ett+2*c6*Ezz))];
dWtt = [c*(exp(Q)*(2*c2*Ett+2*c4*Err+2*c5*Ezz))];
dWzz = [c*(exp(Q)*(2*c3*Ezz+2*c5*Ett+2*c6*Err))];
%
rhooint(j,:) = linspace(ri(j),ra(j),100);

int1 = vpa((F22^2*dWtt-F11^2*dWrr)*(rho)^(-1),10);
int2 = vectorize(int1);
for i = 1:length(rhooint)
Trr(j,i) = quadl(int2,ri(j),rhooint(j,i));
end

Trr_x = F11^2*dWrr;
Trrx(j,:) = subs(Trr_x,'rho',rhooint(j,:));
lm(j,:) = -Trr(j,:) + Trrx(j,:);
Ttt_x = F22^2*dWtt;
Tttx(j,:) = subs(Ttt_x,'rho',rhooint(j,:));
Ttt(j,:) = -lm(j,:) + Tttx(j,:);
Trr(j,:) = -lm(j,:) + Trrx(j,:);
end

for j = 1:3
figure
plot(rhooint(j,:),Trr(j,:),'k')

```

```

hold on
plot(rhoint(j,:),Ttt(j,:),'m')

y(j,:)= (rhoint(j,:)-r_mid(j)).*(Ttt(j,:));
Moment(j) = trapz(rhoint(j,:),y(j,:))
Force(j)=trapz(rhoint(j,:),Ttt(j,:))
end
eps = .02 * theta0
%for j = 1:length(ri)
% for k = 1:length(rhoint)
% error(j,k) = abs(Ttt(j,k) - 0);
% if error(j,k) < eps
%     r_zero(j) = rhoint(j,k)
%     break
% end
% end
%end

if Force(2) > 0
    coefs=polyfit(r_mid(2:3),Force(2:3),1);
    r_nuet=-coefs(2)/coefs(1)
end
if Force(2) < 0
    coefs=polyfit(r_mid(1:2),Force(1:2),1);
    r_nuet=-coefs(2)/coefs(1)
end
if Force(2) == 0;
    r_nuet=r_mid(2)
end

r_mid=r_nuet;

th = Ra - Ri
r_mid = [r_mid+.01*th r_mid-.01*th]

% r = sqrt(theta*(theta0*Ra^2 - theta0*Ri^2 + theta*ri^2)) / theta
for i= 1:3
ri(i) = sqrt(theta*(theta0*Ri^2 - theta0*Ra^2 + theta*r_mid(i)^2)) / theta;
end
%ri = eval(ri)
for i = 1:3
    ra(i) = sqrt(theta*(theta0*Ra^2 - theta0*Ri^2 + theta*r_mid(i)^2)) /
theta;
end

for j = 1:length(ri)

```



```

% Using the given variables, the deformation gradient is calculated as
% follows:
% F = [(theta0*R)/(theta*rho) 0 0; 0 (theta*rho)/(theta0*R) 0; 0 0 1];
F11 = (theta0*Ra)/(theta*rho);
F22 = (theta*rho)/(theta0*Ra);
F33 = lambda;

% Green Strain
Err = 0.5*[F11^2- 1];
Ett = 0.5*[F22^2- 1];
Ezz = 0.5*[F33^2- 1];

Q = c1*(Err^2)+c2*(Ett^2)+c3*(Ezz^2)+2*c4*Err*Ett+2*c5*Ett*Ezz+2*c6*Ezz*Err;
% W = c*(exp(Q)-1);
dWrr = [c*(exp(Q)*(2*c1*Err+2*c4*Ett+2*c6*Ezz))];
dWtt = [c*(exp(Q)*(2*c2*Ett+2*c4*Err+2*c5*Ezz))];
dWzz = [c*(exp(Q)*(2*c3*Ezz+2*c5*Ett+2*c6*Err))];
%
rho(j,:) = linspace(ri(j),ra(j),100);
int1 = vpa((F22^2*dWtt-F11^2*dWrr)*(rho)^(-1),10);
int2 = vectorize(int1);
for i = 1:length(rho)
Trr(j,i) = quadl(int2,ri(j),rho(j,i));
end

Trr_x = F11^2*dWrr;
Trrx(j,:) = subs(Trr_x,'rho',rho(j,:));
lm(j,:) = -Trr(j,:) + Trrx(j,:);
Ttt_x = F22^2*dWtt;
Tttx(j,:) = subs(Ttt_x,'rho',rho(j,:));
Ttt(j,:) = -lm(j,:) + Tttx(j,:);
Trr(j,:) = -lm(j,:) + Trrx(j,:);
end

for j = 1:length(ri)
figure
plot(rho(j,:),Trr(j,:),'k')
hold on
plot(rho(j,:),Ttt(j,:),'m')

y(j,:) = (rho(j,:)-r_mid(j)).*(Ttt(j,:));
Moment(j) = trapz(rho(j,:),y(j,:));
Force(j) = trapz(rho(j,:),Ttt(j,:));
end
eps = .02 * theta0
%for j = 1:length(ri)

```

```

% for k = 1:length(rhoint)
%   error(j,k) = abs(Ttt(j,k) - 0);
%   if error(j,k) < eps
%       r_zero(j) = rhoint(j,k)
%       break
%   end
% end
%end
figure
if Force(2) > 0
    coefs=polyfit(r_mid(2:3),Force(2:3),1);
    r_nuet=-coefs(2)/coefs(1)
end
if Force(2) < 0
    coefs=polyfit(r_mid(1:2),Force(1:2),1);
    r_nuet=-coefs(2)/coefs(1)
end
if Force(2) == 0;
    r_nuet=r_mid(2)
end
plot(r_mid,Force);hold on; plot(r_nuet,0,'x')
%%%%%%%%%%%%%%%%%%%%%%%%%%%%%%%%%%%%%%%%%%%%%%%%%%%%%%%%%%%%%%%%%%%%%%%%
%%%%%%%%%%%%%%%%%%%%%%%%%%%%%%%%%%%%%%%%%%%%%%%%%%%%%%%%%%%%%%%%%%%%%%%%
%

if exist('5_29momcurv_uncut.mat')
    load 5_29momcurv_uncut
    config=size(data_struct,1)+1;
else
    config=1;
    data_struct=[];
end

ri = sqrt(theta*(theta0*Ri^2 - theta0*Ra^2 + theta*r_nuet^2)) / theta;
ra = sqrt(theta*(theta0*Ra^2 - theta0*Ri^2 + theta*r_nuet^2)) / theta;

% Using the given variables, the deformation gradient is calculated as
% follows:
% F = [(theta0*R)/(theta*rho) 0 0; 0 (theta*rho)/(theta0*R) 0; 0 0 1];
F11_n = (theta0*Ra)/(theta*rho);
F22_n = (theta*rho)/(theta0*Ra);
F33_n = lambda;

% Green Strain
Err_n = 0.5*[F11_n^2- 1];

```

```

Ett_n = 0.5*[F22_n^2- 1];
Ezz_n = 0.5*[F33_n^2- 1];

Q_n
=c1*(Err_n^2)+c2*(Ett_n^2)+c3*(Ezz_n^2)+2*c4*Err_n*Ett_n+2*c5*Ett_n*Ezz_n+2*
c6*Ezz_n*Err_n;
% W= c(exp(Q)-1);
dWrr_n= [c*(exp(Q)*(2*c1*Err_n+2*c4*Ett_n+2*c6*Ezz_n))];
dWtt_n= [c*(exp(Q)*(2*c2*Ett_n+2*c4*Err_n+2*c5*Ezz_n))];
dWzz_n= [c*(exp(Q)*(2*c3*Ezz_n+2*c5*Ett_n+2*c6*Err_n))];

rhoht=linspace(ri,ra,100);
int1_n=vpa((F22_n^2*dWtt_n-F11_n^2*dWrr_n)*(rho)^(-1),10);
int2_n=vectorize(int1_n);
for i=1:length(rhoht)
Trr_n(i) =quadl(int2_n,ri,rhoht(i));
end

Trr_xn = F11_n^2*dWrr_n;
Trrx_n = subs(Trr_xn,'rho',rhoht);
lm_n = -Trr_n + Trrx_n;
Ttt_xn = F22_n^2*dWtt_n;
Ttt_n = subs(Ttt_xn,'rho',rhoht);
Ttt_n = -lm_n + Ttt_n;
Trr_n = -lm_n + Trrx_n;

figure
plot(rhoht,Trr_n,'k')
hold on
plot(rhoht,Ttt_n,'m')

y_n= (rhoht-r_nuet).*(Ttt_n);
Moment = trapz(rhoht,y_n)
curvature = 1/ r_nuet
Force=trapz(rhoht,Ttt_n)

temp = input('save?? Y or N')
if strcmp(temp,'Y')
data_struct=[data_struct; curvature Moment Force]
save 5_29momcurv_uncut data_struct
save 5_29momcurv_uncut.txt data_struct -ascii
elseif strcmp(temp,'N')
data_struct=[data_struct]

```

```
end  
C = data_struct(:,1);  
M = data_struct(:,2);  
F = data_struct(:,3);  
  
% figure  
% plot(curvature, moment, 'c')
```

```
</div>
```

```

<div class="moz-text-flowed" style="font-family: -moz-fixed">clear all
close all

%List of given constants for Fung model
c = 22.4; % in kPa
c1= 0.0499;
c2= 1.0672;
c3= 0.4775;
c4= 0.0042;
c5= 0.0903;
c6= 0.0585;

%List of defined variables
Ri=22.4215e-3; %Inner ref radius in meters for cut artery (intact Ri =
22.9885e-3)
Ra = 24.8215e-3; % Outer ref radius in meters for cut artery (intact Ra =
25.3885e-3)
% Ri = 22.9885e-3
% Ra = 25.3885e-3

Lngth=50.23e-3; %1.6*(0.0254); % 1.6 inches times 0.0254 m per inch
lamz=1; %axial stretch set to unity
Q_tot=30.9487*pi/180; %total ref angel

H_tot=Ra-Ri; %total thickness
R_mid=0.5*(Ra+Ri); %ref radius of mid
A_mid=Q_tot*R_mid; %ref arc length of mid

kap_mid_vec=(-0.1:0.01:0.15)*1000; %curvature of mid shell (units of m^-1)
for differencnt configs
q_tot_vec=kap_mid_vec*A_mid; %total angle of the configs

%this program models the wall as 100 thin shells with i indicating nodes
%between the shells (goes from i=1 on inner to i=101 on outer boundary).
%The shells themselves are indicated by j with j=1 the inner shell and
%j=100 as the outer shell.
R_i=(0:100)*H_tot/100+Ri; %ref radius between the shells
A_i=Q_tot*R_i; %ref arc length between the shells
R_j=0.5*(R_i(1:100)+R_i(2:101)); %ref radius of shells
H_j=-R_i(1:100)+R_i(2:101); % ref thickness of shells
A_j=Q_tot*R_j; % ref arc length of shells

kap_in=0*q_tot_vec; %initialize curvature data vector
M=0*q_tot_vec; %initialize Moment data vector

%loop over the configurations given by the q_tot_vec

```

```

for i_cnfg = 1:max(size(M))
    i_cnfg %displays i_cnfg value on command window line
    figure(1);plot(1,0,'+');hold on %place a plus symbol at the point
indicating
    %unit hoop stretch for middle and zero net hoop stress
    %this figure will be used to visualize convergence on a config with the
    %correct q_tot and nearly zero net hoop stress
    ylabel('sum of hoop stress*thickness')
    xlabel('hoop stretch of middle')

    q_tot=q_tot_vec(i_cnfg); %the total angle of current config
    lamq_mid=1; % start with hoop stretch of 1 for middle

    a_mid=lamq_mid*A_mid; %arc length of middle
    lamq_mid_1=lamq_mid; %save value of first guess for lamq_mid in the
variable lamq_mid_1

    a_i=sqrt(a_mid^2-(A_mid^2-A_i.^2)*q_tot/Q_tot); %arc length between
the shells
    a_j=0.5*(a_i(1:100)+a_i(2:101)); %arc length at center of shells
    kap_i=q_tot./a_i; %curvature between the shells
    kap_j=q_tot./a_j; %curvature at center of shells
    h_j=A_j.*H_j./a_j; %thickness of shells
    lamq_i=a_i./A_i; %hoop stretch between the shells
    lamq_j=a_j./A_j; %hoop stretch at the center of shells

    %calculate strain components at nodes between shells
    Err = 0.5*[lamq_i.^(-2)/lamz^2- 1];
    Eqq = 0.5*[lamq_i.^2- 1];
    Ezz = 0.5*[lamz^2- 1];

    %calculate derivatives of W at nodes between shells
    Q
=c1*(Err.^2)+c2*(Eqq.^2)+c3*(Ezz.^2)+2*c4*Err.*Eqq+2*c5*Eqq.*Ezz+2*c6*Ezz.*Er
r;
    % W= c*(exp(Q)-1);
    dWrr_i= [c*(exp(Q).*(2*c1*Err+2*c4*Eqq+2*c6*Ezz))];
    dWqq_i= [c*(exp(Q).*(2*c2*Eqq+2*c4*Err+2*c5*Ezz))];
    dWzz_i= [c*(exp(Q).*(2*c3*Ezz+2*c5*Eqq+2*c6*Err))];

    %calculate the components of extra stress at the nodes between
    %shells (i) and at the center of shells (j)
    Trr_ie=dWrr_i./lamz^2*lamq_i.^2;
    Tqq_ie=dWqq_i.*lamq_i.^2;
    Tzz_ie=dWzz_i*lamz^2;
    Trr_je=0.5*(Trr_ie(1:100)+Trr_ie(2:101));

```

```

Tqq_je=0.5*(Tqq_je(1:100)+Tqq_je(2:101));
Tzz_je=0.5*(Tzz_je(1:100)+Tzz_je(2:101));

%get dTrr/dr for each shell
dTrrdr_j=kap_j.*(Tqq_je-Trr_je);
Trr_i=0*Trr_je;

%get Trr for node (si+1) based on Trr for node (si) and the
%dTrr/dr for the shell between node (si) and node (si+1)
for si=1:100
    Trr_i(si+1)=dTrrdr_j(si)*h_j(si)+Trr_i(si);
end
%get pressure like Lagrange multiplier ppress
ppres=Trr_je-Trr_i;

%calculate the stresses
Tqq_i=-ppres+Tqq_je;
Tzz_i=-ppres+Tzz_je;
Trr_j=0.5*(Trr_i(1:100)+Trr_i(2:101));
Tqq_j=0.5*(Tqq_i(1:100)+Tqq_i(2:101));
Tzz_j=0.5*(Tzz_i(1:100)+Tzz_i(2:101));

%sum the hoop stress times the shell thickness
sTqq=sum(Tqq_j.*h_j)
sTqq_1=sTqq;
plot(lamq_mid,sTqq_1,'x');hold on

% while loop to converge on config with correct q_tot but with a net
% hoop stress that is nearly null
while abs(sTqq) > 0.00001

    lamq_mid_1=lamq_mid; %save prior value of lamq_mid
    sTqq_1=sTqq; %save prior value of sTqq
    y_shift=-sTqq_1/100; %divide the net by the number of shells to get
shift
    % of each shell to yield null net hoop stress then find the lamq
    % shift that would give the y-shift assuming Tqq versus shell
    % number was a linear relation with slope given by the values of
    % the 50 and 51st shells

    lamq_shift=y_shift*(lamq_j(51)-lamq_j(50))/(Tqq_j(51)*h_j(51)-Tqq_j(50)*h_j(50));

    lamq_mid=lamq_mid+lamq_shift; %shift lamq of middle
    a_mid=lamq_mid*A_mid; %recalculate arc length of middle
    lamq_mid_2=lamq_mid; %save this new value of arc length

```

```

a_i=sqrt(a_mid^2-(A_mid^2-A_i.^2)*q_tot/Q_tot); %arc length between
the shells
a_j=0.5*(a_i(1:100)+a_i(2:101)); %arc length at center of shells
kap_i=q_tot./a_i; %curvature between the shells
kap_j=q_tot./a_j; %curvature at center of shells
h_j=A_j.*H_j./a_j; %thickness of shells
lamq_i=a_i./A_i; %hoop stretch between the shells
lamq_j=a_j./A_j; %hoop stretch at the center of shells

%calculate strain components at nodes between shells
Err = 0.5*[lamq_i.^(-2)/lamz^2- 1];
Eqq = 0.5*[lamq_i.^2- 1];
Ezz = 0.5*[lamz^2- 1];

%calculate derivatives of W at nodes between shells
Q
=c1*(Err.^2)+c2*(Eqq.^2)+c3*(Ezz.^2)+2*c4*Err.*Eqq+2*c5*Eqq.*Ezz+2*c6*Ezz.*Er
r;
% W= c*(exp(Q)-1);
dWrr_i=[c*(exp(Q).*(2*c1*Err+2*c4*Eqq+2*c6*Ezz))];
dWqq_i=[c*(exp(Q).*(2*c2*Eqq+2*c4*Err+2*c5*Ezz))];
dWzz_i=[c*(exp(Q).*(2*c3*Ezz+2*c5*Eqq+2*c6*Err))];

%calculate the components of extra stress at the nodes between
%shells (i) and at the center of shells (j)
Trr_ie=dWrr_i./(lamz^2*lamq_i.^2);
Tqq_ie=dWqq_i.*lamq_i.^2;
Tzz_ie=dWzz_i.*lamz^2;
Trr_je=0.5*(Trr_ie(1:100)+Trr_ie(2:101));
Tqq_je=0.5*(Tqq_ie(1:100)+Tqq_ie(2:101));
Tzz_je=0.5*(Tzz_ie(1:100)+Tzz_ie(2:101));

%get dTrr/dr for each shell
dTrrdr_j=kap_j.*(Tqq_je-Trr_je);
Trr_i=0*Trr_ie;

%get Trr for node (si+1) based on Trr for node (si) and the
%dTrr/dr for the shell between node (si) and node (si+1)
for si=1:100
    Trr_i(si+1)=dTrrdr_j(si)*h_j(si)+Trr_i(si);
end
%get pressure like Lagrange multiplier ppress
ppres=Trr_ie-Trr_i;

%calculate the stresses
Tqq_i=-ppres+Tqq_ie;

```



```

Tzz_i=-ppres+Tzz_ie;
Trr_j=0.5*(Trr_i(1:100)+Trr_i(2:101));
Tqq_j=0.5*(Tqq_i(1:100)+Tqq_i(2:101));
Tzz_j=0.5*(Tzz_i(1:100)+Tzz_i(2:101));

%sum the hoop stress times the shell thickness
sTqq=sum(Tqq_j.*h_j)
sTqq_2=sTqq;
plot(lamq_mid,sTqq_2,'o');hold on

%hoop stretch at the middle which will hopefully yeild sTqq as zero
%is calculated by interpolating from prior two guesses
lamq_mid=(sTqq_2*lamq_mid_1-sTqq_1*lamq_mid_2)/(sTqq_2-sTqq_1);
a_mid=lamq_mid*A_mid; %arc length at the middle
lamq_mid_3=lamq_mid;

a_i=sqrt(a_mid^2-(A_mid^2-A_i.^2)*q_tot/Q_tot); %arc length between
the shells
a_j=0.5*(a_i(1:100)+a_i(2:101)); %arc length at center of shells
kap_i=q_tot./a_i; %curvature between the shells
kap_j=q_tot./a_j; %curvature at center of shells
h_j=A_j.*H_j./a_j; %thickness of shells
lamq_i=a_i./A_i; %hoop stretch between the shells
lamq_j=a_j./A_j; %hoop stretch at the center of shells

%calculate strain components at nodes between shells
Err = 0.5*[lamq_i.^(-2)/lamz^2- 1];
Eqq = 0.5*[lamq_i.^2- 1];
Ezz = 0.5*[lamz^2- 1];

%calculate derivatives of W at nodes between shells
Q
=c1*(Err.^2)+c2*(Eqq.^2)+c3*(Ezz.^2)+2*c4*Err.*Eqq+2*c5*Eqq.*Ezz+2*c6*Ezz.*Er
r;
% W= c*(exp(Q)-1);
dWrr_i= [c*(exp(Q).*(2*c1*Err+2*c4*Eqq+2*c6*Ezz))];
dWqq_i= [c*(exp(Q).*(2*c2*Eqq+2*c4*Err+2*c5*Ezz))];
dWzz_i= [c*(exp(Q).*(2*c3*Ezz+2*c5*Eqq+2*c6*Err))];

%calculate the components of extra stress at the nodes between
%shells (i) and at the center of shells (j)
Trr_ie=dWrr_i./(lamz^2*lamq_i.^2);
Tqq_ie=dWqq_i.*lamq_i.^2;
Tzz_ie=dWzz_i*lamz^2;
Trr_je=0.5*(Trr_ie(1:100)+Trr_ie(2:101));
Tqq_je=0.5*(Tqq_ie(1:100)+Tqq_ie(2:101));

```

```

Tzz_je=0.5*(Tzz_ie(1:100)+Tzz_ie(2:101));

%get dTrr/dr for each shell
dTrrdr_j=kap_j.*(Tqq_je-Trr_je);
Trr_i=0*Trr_ie;

%get Trr for node (si+1) based on Trr for node (si) and the
%dTrr/dr for the shell between node (si) and node (si+1)
for si=1:100
    Trr_i(si+1)=dTrrdr_j(si)*h_j(si)+Trr_i(si);
end
%get pressure like Lagrange multiplier ppress
ppres=Trr_ie-Trr_i;

%calculate the stresses
Tqq_i=-ppres+Tqq_ie;
Tzz_i=-ppres+Tzz_ie;
Trr_j=0.5*(Trr_i(1:100)+Trr_i(2:101));
Tqq_j=0.5*(Tqq_i(1:100)+Tqq_i(2:101));
Tzz_j=0.5*(Tzz_i(1:100)+Tzz_i(2:101));

%sum the hoop stress times the shell thickness
sTqq=sum(Tqq_j.*h_j)
sTqq_3=sTqq;
plot(lamq_mid,sTqq_3,'.');hold on

%connect the dots on the last three calculations of sTqq to
%visualize the convergence
plot([lamq_mid_1 lamq_mid_2 lamq_mid],[sTqq_1 sTqq_2 sTqq_3])
end % end while loop for reducing abs(sTqq) to below the set level

dtmp=0*a_i; % temporary distance vector that will be zero on inner wall
and increases to outer
for sj=1:100
    dtmp(sj+1)=sum(h_j(1:sj));
end
% l_arm_j is vector of lever arm of moment of each shell with center
% being zero (i.e. zero is between shells 50 and 51)
l_arm_j=0.5*(dtmp(1:100)+dtmp(2:101))-dtmp(51);
% calculate Moment M for the config associated with i_cnfg value
M(i_cnfg)=lamz*Lngh*sum(Tqq_j.*h_j.*l_arm_j);
% calculate curvature of inner wall for the config associated with
i_cnfg value
kap_in(i_cnfg)=q_tot/a_i(1);

end % end loop for i_cnfg

```

```
figure;  
%plot the moment versus curvature of inner wall  
%the division by 1000 makes curvature in 1/mm instead of 1/m  
%the multiplication by 1000000 makes M in mN*mm instead of N*m  
plot(kap_in/1000,M*1000000,'o');  
hold on;  
plot(kap_in/1000,M*1000000)  
hold on;  
errorbar(kap_in/1000,M*1000000,.025*ones(size(kap_in)));  
ylabel('Moment (mN*mm)')  
xlabel('Curvature of Luminal Wall (1/mm)')  
  
</div>
```

```

<div class="moz-text-flowed" style="font-family: -moz-fixed">
clear all
close all

%Allows user to input image filename.
%filename = input('Input image filename now.')
filename = ['H:\4_18_06_ovine\artery360_cut.bmp'];
I = imread(filename);
imagesc(I); hold on

if exist('error1.mat')
    load error1
    image_num=size(data_struct,1)+1;
else
    image_num=1;
    data_struct=[];
end

xdcr_top_displacement=input('input the displacment of top of transducer in
degrees')*pi/180;

%Allows user to pick points on boundary of cell.
junk_input=input('zoom image to pick the points on reference object then
press enter');
ref_pts_in=[];
for i=1:2
    in_pt = round(ginput(1));
    if isempty(in_pt) == 0
        plot(in_pt(1),in_pt(2),'r+');
        ref_pts_in=[ref_pts_in in_pt];
    else
        error('two references points are needed')
    end
end

junk_input=input('zoom image to pick the points on torque transducer then
press enter');
xdcr_pts_in=[];
for i=1:2
    in_pt = round(ginput(1));
    if isempty(in_pt) == 0
        plot(in_pt(1),in_pt(2),'g+');
        xdcr_pts_in=[xdcr_pts_in in_pt];
    else
        error('two references points are needed')
    end
end

```

```

end

junk_input=input('zoom image to pick the points on reference pins then press
enter');
pin_pts_in=[];
for i=1:4
    in_pt = round(ginput(1));
    if isempty(in_pt) == 0
        plot(in_pt(1),in_pt(2),'c+');
        pin_pts_in=[pin_pts_in in_pt];
    else
        error('two references points are needed')
    end
end
pin1 = pin_pts_in(:,2) - pin_pts_in(:,1) ;
pin2 = pin_pts_in(:,4) - pin_pts_in(:,3) ;
theta = subspace(pin1,pin2) * 180/pi

junk_input=input('zoom image to pick the points on artery then press
enter');
'click on points in figure and press enter when done'
ring_pts_in=[];
in_pt=[4; 0];
pts_in=[];
while isempty(in_pt) == 0
    in_pt = round(ginput(1));
    if isempty(in_pt) == 0
        plot(in_pt(1),in_pt(2),'b. ');
        ring_pts_in=[ring_pts_in in_pt];
    end
end
ring_pts_in
ref_pts_in = [ref_pts_in(1,1) ref_pts_in(1,2);ref_pts_in(2,1)*-1
ref_pts_in(2,2)*-1];
ref_vec=ref_pts_in(:,2)-ref_pts_in(:,1)
ref_vec_lngth=sqrt(ref_vec*ref_vec)
mag_factor=6/ref_vec_lngth
lab_ref_angle=atan2(ref_vec(2),ref_vec(1))
xdcr_pts_in = [xdcr_pts_in(1,1) xdcr_pts_in(1,2);xdcr_pts_in(2,1)*-1
xdcr_pts_in(2,2)*-1];
xdcr_vec=xdcr_pts_in(:,2)-xdcr_pts_in(:,1)
xdcr_bottom_angle=atan2(xdcr_vec(2),xdcr_vec(1))-lab_ref_angle

% start_up=input('label three points on artery p1 p2 p3 with p2 as the
middle point')

```

```

p1=ring_pts_in(:,1);
p2=ring_pts_in(:,2);
p3=ring_pts_in(:,3);

% we now think of two lines from p1 to p2 and from p2 to p3...we want the
% slope of those lines

m1=(p2(2,1)-p1(2,1))/(p2(1,1)-p1(1,1));

m2=(p3(2,1)-p2(2,1))/(p3(1,1)-p2(1,1));

% once you have the slopes of the line, you solve for equations of the
% perpendicular lines that would intersect eachother at the center of the
% circle. The perpendicular lines should start from the midpoint of the
% vector p2-p1 and the vector p3-p2. Once you have the equations of the
% perpendicular lines, set them equal to each other and solve for x. Once
% x is known, plug back into the perpendicular lines and solve for y. This
% is the center of the circle.
%
warning off MATLAB:dividebyzero
xc=
(m1*m2*(p1(2,1)-p3(2,1))+m2*(p1(1,1)+p2(1,1))-m1*(p2(1,1)+p3(1,1)))/(2*(m2-m1));

yc= -1/m1*(xc-((p2(1,1)+p1(1,1))/2))+((p2(2,1)+p1(2,1))/2);
center=[xc;yc]

%now pick any point to solve for the radius of the circle (as is p1 is
%used)

r=sqrt((p1(1,1)-center(1,1))^2+(p1(2,1)-center(2,1))^2)*mag_factor

curvature= 1/r
temp=input('to save type Y or to not save type N')
if strcmp(temp,'Y')
data_struct=[data_struct; curvature xdcr_bottom_angle xdcr_top_displacement
theta]
save error1 data_struct
save error1 data_struct -ascii
elseif strcmp(temp,'N')
data_struct=[data_struct]
end

</div>

```

```

<div class="moz-text-flowed" style="font-family: -moz-fixed">%%%%%%%%%
THICKNESS
clear all
clc

filename = ['H:\4_18_06_ovine\reference.bmp'];
I = imread(filename);
imagesc(I); hold on

% if exist('thickness.mat')
%   load thickness
%   image_num=size(data_struct,1)+1;
% else
%   image_num=1;
%   data_struct=[];
% end

junk_input=input('zoom image to pick the points on reference ruler then
press enter');
ref_pts_in=[];
for i=1:2
    in_pt = round(ginput(1));
    if isempty(in_pt) == 0
        plot(in_pt(1),in_pt(2),'r+');
        ref_pts_in=[ref_pts_in in_pt];
    else
        error('two references points are needed')
    end
end

ref_vec=ref_pts_in(:,2)-ref_pts_in(:,1);
ref_vec_lngth=sqrt(ref_vec'*ref_vec);
mag_factor=6/ref_vec_lngth;

junk_input=input('zoom image to pick the points for Rin and Ra vector');
pin_pts_in=[];
for i=1:4
    in_pt = round(ginput(1));
    if isempty(in_pt) == 0
        plot(in_pt(1),in_pt(2),'c+');
        pin_pts_in=[pin_pts_in in_pt];
    else
        error('two references points are needed')
    end
end
Rin_vec = pin_pts_in(:,2) - pin_pts_in(:,1);

```

```
Ra_vec = pin_pts_in(:,4) - pin_pts_in(:,3);  
Rin_len = sqrt(Rin_vec'*Rin_vec);  
Ra_len = sqrt(Ra_vec'*Ra_vec);  
  
Thickness = (Ra_len - Rin_len)* mag_factor  
</div>
```


VITA

Gabriel Alejandro Reza received his Bachelor of Science in biomedical engineering at Arizona State University in 2004. He entered into the Master's program at Texas A&M University in Fall 2004. He received his Master of Science in biomedical engineering in August 2006. His research interest are soft-tissue mechanics at the aggregate level, and he has taken a job with St. Jude Medical. Mr. Reza can be reached at 320 East 54th St. #3F, New York NY, 10022. His email address is lilgabee2@aol.com.